



Cycle 26 COS/FUV Spectroscopic Sensitivity Monitor

Ravi Sankrit¹

¹ Space Telescope Science Institute, Baltimore, MD

1 September 2020

ABSTRACT

The Cycle 26 COS/FUV spectroscopic sensitivity monitor ran from December 2018 to November 2019. The standard mode observations were obtained at Lifetime Position 4 (LP4), the nominal position for COS starting October 2, 2017, and the blue modes (G130M/1055 and G130M/1096) were obtained at Lifetime Position 2 (LP2). The new modes introduced in Cycle 26 (G130M/1533 and G140L/800) were included in the monitoring observations starting in February 2019. The Time-Dependent Sensitivity (TDS) slopes of the standard and blue modes were found to remain steady, and range from 0% to -4% per year. The TDS slopes of the new cenwaves 1533 and 800 were calculated from the data obtained in this program. In this ISR we describe the program and its execution, and provide a summary of the analysis and results.

Contents

1. Introduction	2
2. Program Design	2
3. Observations	4
4. Analysis and Results	5
4.1 Regular TDS Monitor	5
4.2 New Cenwaves TDSTAB	7
5. Reference Files Delivered	9

6. Continuation Plan	9
Change History for COS ISR 2020-06	9
References	9

1. Introduction

The initial discovery of declines in sensitivity in several COS spectroscopic modes was reported by Osten et al. (2010). Monitoring programs were initiated to follow these trends. The Far-Ultraviolet (FUV) Time-Dependent Sensitivity (TDS) monitoring programs, and their results have been described in a series of publications (Osten et al. 2011, Bostroem et al. 2014, De Rosa et al. 2016, 2017, 2018, Sankrit 2019). The temporal sensitivity variations are modeled as functions of wavelength for each combination of grating (G130M, G160M, G140L) and segment (FUVA, FUVB). These are included in the TDS reference file, TDSTAB, which is used in CalCOS in association with the photometric throughput reference file, FLUXTAB, to obtain flux calibrated data.

The Cycle 26 FUV TDS monitor (PID: 15535, PI: R. Sankrit) consisted of observations of the flux calibration standards, GD71 and WD0308-565, with the plan of obtaining data every two months between December 2018 and November 2019.

2. Program Design

The FUV TDS program is designed to obtain regular observations of flux calibration standards using the shortest and longest central wavelength standard settings of each grating, and additionally G130M/1222 (first offered to the community in Cycle 20), and the “blue modes”, G130M/1055 and G130M/1096. Two modes, the “new cenwaves”, G160M/1533 and G140L/800 were introduced at the beginning of Cycle 26 and were added to the regularly monitored modes starting with the second set of visits, obtained in February and March, 2019. G160M/1533 uses both detector segments, while G140L/800 uses only segment FUVA.

The two white dwarf standards, GD71 and WD0308-565, have been used for the FUV TDS monitor since the move to LP2 in Cycle 20. The choice of target for each cenwave and segment is based on optimizing the signal-to-noise ratio (S/N) achieved, while minimizing the impact on detector lifetime.

The exposure times were determined by requiring a S/N of 15 per resel at the wavelength of least sensitivity for all the standard modes, except G130M/1222, and for the new cenwave G140L/800. For the blue modes and for G130M/1222, the goal was to obtain $S/N \sim 25$ per resel at the wavelength of maximum sensitivity, which ensured that $S/N > 15$ for $\lambda > 1030 \text{ \AA}$ for G130M/1096/FUVB, and for $\lambda > 1130 \text{ \AA}$ for G130M/1055/FUVA and G130M/1222. For G140L/800, the goal was to obtain S/N of 15 per resel at the wavelength of least sensitivity longward of 1150 Å. Below this

Table 1. Modes Tracked using GD71

Grating	Cenwave	Segment	t_{exp} (sec)
G130M	1096	B	744
G160M	1533	A	103
	1577	A	132
	1623	A	172

Table 2. Modes Tracked using WD0308-565

Grating	Cenwave	Segment	t_{exp} (sec)
G130M	1055	A	363
	1222	both	254
	1291	both	233
	1327	A	278
G160M	1533	B	222
	1577	B	273
	1623	B	369
G140L	800	A	363
	1105	A	327
	1280	both	328

threshold the throughput is low because of the sharp drop in reflectivity of the HST MgF₂/Al primary mirror. The exposure time used for this setting provides S/N of between 30 and 40 per 20Å bin at these wavelengths.

The resulting total exposure times, plus overheads require two orbits per visit for GD71 and three orbits per visit for WD0308-565. Since there are no lamp lines available in the wavelength range covered by G130M/1096/FUVB, the GD71 visits include a wavelength calibration lamp observation through 1096/FUVA that is obtained immediately after the science exposure, at the same Optics Select Mechanism 1 (OSM1) position.

The modes tracked in the Cycle 26 program with GD71 and WD0308-565, and the exposure times used are listed in Tables 1 and 2, respectively. The exposure times are close to those used in Cycle 25. In the earlier program, without the new cenwaves, one fewer orbit was required for each visit, and the exposure times were allowed to increase to pack the orbits. In Cycle 26 the exposure times determined from the ETC calculations were used without any adjustment. The mode G130M/1327/FUVB, which

Table 3. Regular Program Observation Dates

Obs. Date	Visit No.	Target
2018-Dec-26	02	GD71
2019-Feb-22	04	GD71
2019-Mar-20	53	WD0308-565
2019-Apr-16	05	WD0308-565
2019-Jun-28	57	WD0308-565
2019-Aug-19	58	WD0308-565
2019-Aug-24	09	GD71
2019-Oct-16	11	GD71
2019-Nov-11	60	WD0308-565

was monitored up until Cycle 24 is not observed any longer as a consequence of the COS 2025 policy (Oliveira et al. 2018).

The visit structure and sequence of observations in the Cycle 26 program follows the “complete monitoring sequence” implemented in Cycle 24 (PID: 14854, PI: G. De Rosa), described in De Rosa (2018), with the addition of the new cenwaves starting with visit 03 in February 2019. Based on the analyses of the Cycle 24 data, it was determined that the “reduced monitoring sequence” (using one orbit every alternate month) was not necessary, and therefore was dropped in the Cycle 25 program.

The standard mode and new cenwave observations were obtained at the nominal (current) COS FUV lifetime position (LP4), while the blue modes are observed at LP2. In all cases, the observations were obtained at FP-POS 3 only.

3. Observations

The data used in the regular FUV TDS analysis were based on the set of observations shown in Table 3, organized by the observation date. The original program included six visits for WD0308-565, and five for GD71, which is not visible between the end of April and the beginning of August. The program was impacted by several failed observations, two of which were not repeated. In one case (visit 01) the repeat observation would have been too close in time to the following planned visit for it to have been worthwhile, and in the second case (visit 06) the target, GD71 was entering its period of non-visibility. Thus the final program consisted of five WD0308-565 visits, and four GD71 visits. All the data from successful observations are available in the archive.

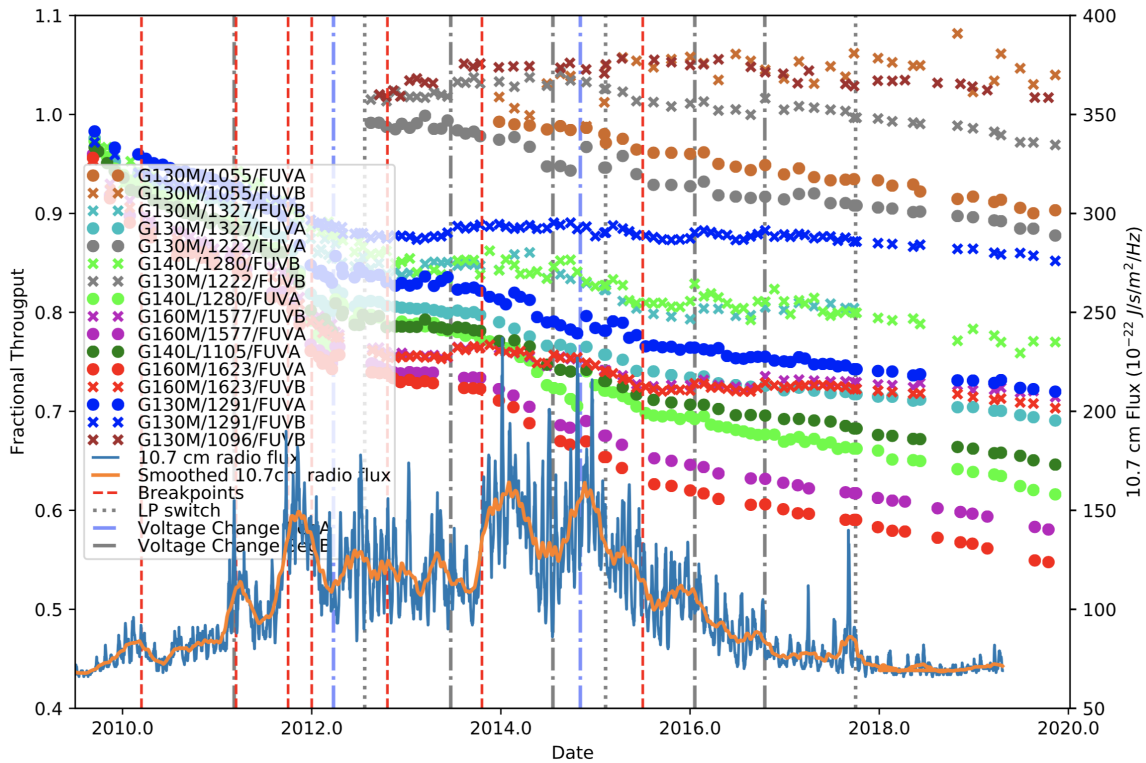


Figure 1. The change in COS FUV spectroscopic sensitivity with time. The fractional throughput, relative to first light, is shown for each mode tracked as a function of decimal year. The solar activity directed at Earth, as measured by the 10.7 cm flux is shown as a solid blue line (overlaid with a smoothed version in orange). Dashed red vertical lines show the breakpoints used in the piecewise linear function that models the TDS. The dates of the LP moves are shown as dotted grey lines, and the dot-dashed lines indicate when the operational voltage was changed.

4. Analysis and Results

4.1 Regular TDS Monitor

The data were analyzed following the method described in Bostroem (2014), and using the script, *cos_tds_analysis.py*. Calibrated *_x1d.fits* files obtained as part of the FUV TDS monitoring programs from 2009 through November 2019 were used in the analysis. The net counts were binned over 5 \AA for the medium resolution modes, and over 20 \AA for the low resolution modes. The data obtained at LP2, LP3, and LP4, are scaled to data obtained at LP1, LP2 and LP3, respectively using contemporaneous observations obtained at the different LPs. The data are fit using a piecewise-linear function with breakpoints at decimal years 2012.20, 2011.20, 2011.75, 2012.00, 2012.80, 2013.80 and 2015.50, the last introduced at the end of Cycle 24 (De Rosa 2018). The overall relative sensitivity is normalized to 1.0 at the time of first light

(May 01, 2009). Fig. 1 shows a summary plot of the sensitivity against time. Also plotted for comparison is the solar activity directed towards the earth as a function of time. The 10.7 cm solar fluxes are obtained periodically from the Space Weather Prediction Center of the National Oceanic and Atmospheric Administration.

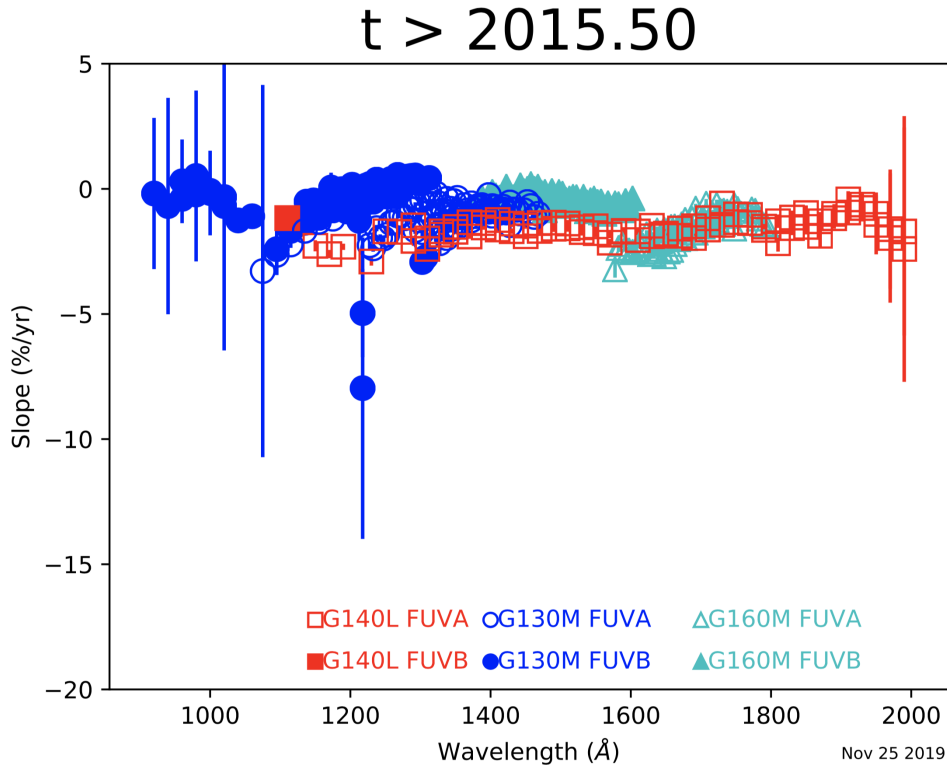


Figure 2. The COS TDS slopes obtained at the end of the regular Cycle 26 observations (November 2019) expressed in percentage change per year plotted against wavelength for the different gratings and segments. Note that the G140L, FUVB slope is a for a single 20 Å bin in the cenwave 1280 setting. The errors on the derived slopes are small except in some cases near the detector edges, and around airglow lines.

The TDS slopes for the linear fits since the last breakpoint (2015.5) are relatively uniform over the COS wavelength range, varying between approximately 0% and -4% per year. In Fig. 2 the TDS slopes are shown plotted against wavelength for each grating and segment.

The absolute and relative flux accuracies remained within 5% and 2%, respectively for all the modes (except for G140L/1280/FUVB, and the blue modes, for which the requirements are less stringent) for most of the duration of Cycle 26. However, for the later visits, systematic divergences were noticeable at the edges of the FUVB detector segment, with the slope becoming steeper at the short-wavelength end, and shallower at the long-wavelength end compared with the TDS model. Therefore, an update was planned, and the process of creating a new TDSTAB reference file is

Table 4. New Cenwave TDSTAB: ROOTNAMES and Observation Dates

Mode	Rootname	Obs. Date
G160M/1533/FUVA	ldsi02u2q	2018-Aug-16
	ldv004u6q	2019-Feb-22
	ldv009axq	2019-Aug-24
	ldv011jtg	2019-Oct-16
G160M/1533/FUVB	ldsi51kaq	2018-Jun-26
	ldv053n0q	2019-Mar-20
	ldv005g8q	2019-Apr-16
	ldv057z1q	2019-Jun-29
G140L/800/FUVA	ldso01ioq	2018-Jun-24
	ldv053n6q	2019-Mar-20
	ldv005gfq	2019-Apr-16
	ldv057zccq	2019-Jun-29
	ldv058btq	2019-Aug-19

currently underway.

4.2 New Cenwaves TDSTAB

The TDS models for the new cenwaves were obtained from Cycle 26 monitoring data, supplemented by data from the original Flux Calibration programs for these modes – PID:15458, PI: E. Frazer for G160M/1533, and PID:15483, PI: R. Sankrit for G140L/800. The rootnames of the data files, and the observation dates are listed in Table 4. The targets used are WD0308-565 for G60M/1533/FUVB and G140L/800, and GD71 for G160M/1533/FUVA (see Tables 1, 2).

The TDS model for each of the new cenwave modes was derived from the net count-rates obtained from the calibrated `_x1d.fits`. Wavelength regions where airglow impacts the spectra were masked out, as were individual locations where the DQ flags were zero. For each new cenwave mode the data were binned and for each bin, the count-rate against time was fit by a straight line. Bin sizes of 5 Å were used for G160M/1533. For G140L/800, bin sizes of 20 Å were used for wavelengths beyond 1115 Å, and the region 915–1115 Å was treated as a single bin because of the low count-rate. These slopes and intercepts were converted to the values used in the TDSTAB which uses a reference time of 2003-Oct-10, and expresses the slopes in units of %-change per year. Then these slopes and intercepts were smoothed by 11 bins, corresponding to 55 Å for the G160M/1533 models and 220 Å for G140L/800, longward of 1115 Å, and then interpolated onto the wavelength grids used in the TDSTAB reference file

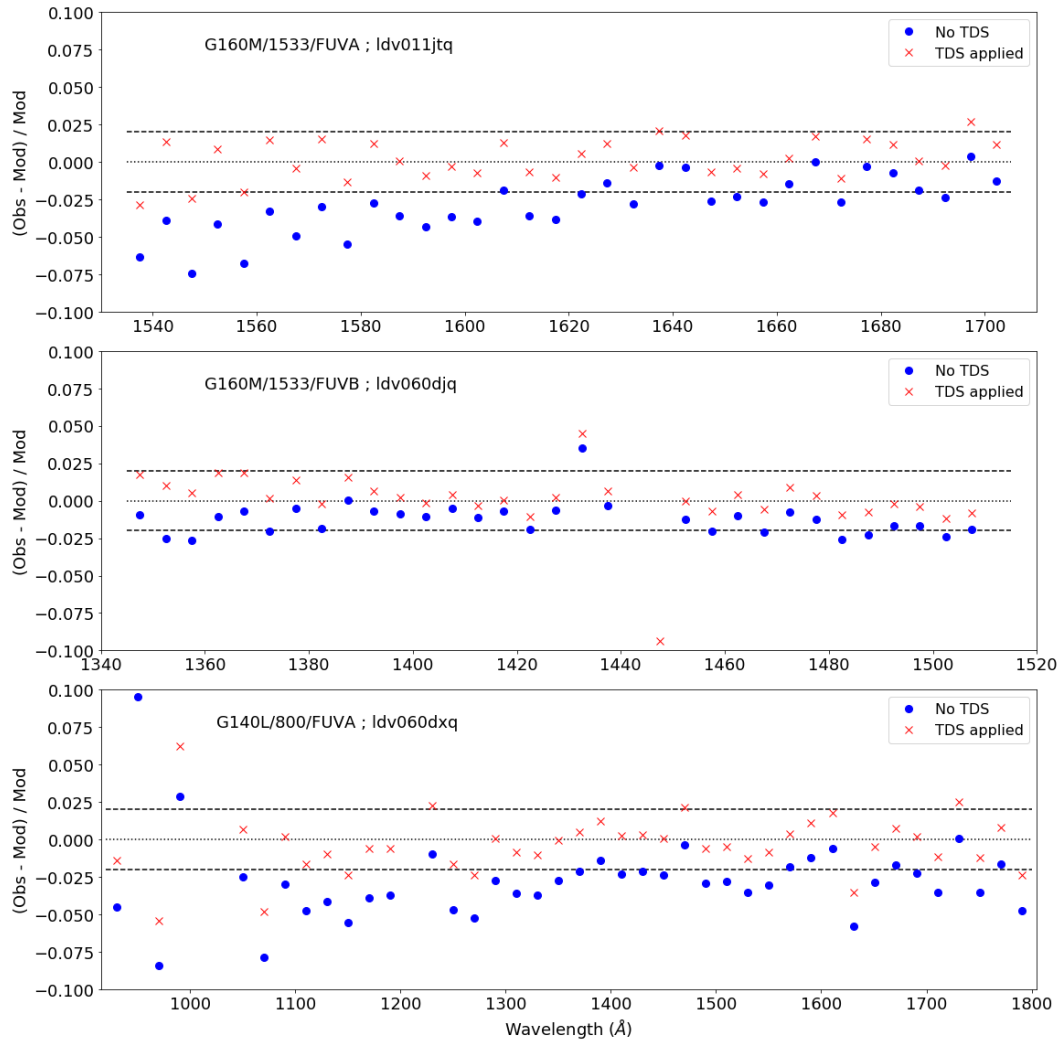


Figure 3. Results of the scientific validation of the new cenwaves TDSTAB. The plots show the fractional residuals of the calibrated fluxes against CALSPEC model spectra `gd71_mod_010.fits`, and `wd0308_565_mod_003.fits`. The mode being tested and the rootname of the data file used are shown in each panel. The blue circles show the case where no TDS correction has been applied, and the red crosses show the results of using the new TDSTAB reference file. In each case the dashed lines mark the nominal 2% tolerance limits.

The scientific validation of the new TDSTAB reference file was done by calibrating data obtained during visits 11 and 60 (Table 3) of the monitoring program using the new file, and comparing the results with the standard pipeline calibration that did not apply any TDS correction. The comparison was done by plotting the fractional residuals of the fluxes compared with the standard star model spectra. The results are shown in Fig. 3. The plots show that the new TDSTAB is generally successful in bringing the fluxes within about 2% of the model. The exceptions to this are in the

short-wavelength region for G140L/800/FUVA where the low count-rates result in larger uncertainties. (We note that the discrepant point around 1450 Å in the case of G160M/1533/FUVB is due to a gain-sag hole that had not as yet been flagged when these data were calibrated.)

5. Reference Files Delivered

The TDSTAB reference file 29o1427fl_tds.fits, applicable for the new cenwaves G160M/1533 and G140L/800, was delivered based on the results outlined in §4.2. The parameters were subsequently incorporated into cenwave-dependent TDSTAB reference file 43n19046l_tds.fits.

6. Continuation Plan

In Cycle 27, the regular monitoring of the FUV TDS continued in program 15773 (PI: R. Sankrit). The targets and frequency of visits are the same as in Cycle 26.

Change History for COS ISR 2020-06

Version 1: 1 September 2020- Original Document

References

- Bostroem, K. A., et al. 2015, COS Technical Instrument Reports 2014-05
- De Rosa, G., Sana, H., Ely, J. and the COS team, 2016, COS Instrument Science Report 2016-13
- De Rosa, G. and the COS team, 2017, COS Instrument Science Report 2017-10
- De Rosa, G. and the COS team, 2018, COS Instrument Science Report 2018-09
- Oliveira, C., et al. 2018, COS Instrument Science Report 2018-16
- Osten, R. A., et al. 2010, COS Instrument Science Report 2010-15
- Osten, R. A., et al. 2011, COS Instrument Science Report 2011-02
- Sankrit, R. 2019, COS Instrument Science Report 2019-18